ACCOUNTING FOR TURBULENCE IN NUMERICAL SIMULATION OF OCEAN CURRENT TURBINE

Parakram Pyakurel[1], James H. VanZwieten and Manhar Dhanak
Florida Atlantic University
Boca Raton, FL, USA

[1]Corresponding author: ppyakurel2014@fau.edu

INTRODUCTION

Ocean current based electricity production has a technically extractable potential of 163 TWh/year in the US [1], which is equivalent to 4% of 2014 US electricity production [2]. Off Florida the time-averaged ocean current energy flux can exceed 3.0 kW/m^2 [3]. Prototypes of Ocean Current Turbine (OCT) have been developed to harness this resource and tested offshore [4]. Numerical simulation to predict performance of OCT using an unsteady Blade Element Momentum (BEM) method has been developed by Southeast National Marine Renewable Energy Center (SNMREC) [5, 6].

This paper presents a method to incorporate turbulence in existing SNMREC numerical simulation to evaluate turbine performance in a more realistic oceanic environment. This methodology is primarily based on the research of [7, 8] in that statistical approach utilizing power spectral density to calculate flow velocities is adopted. However, analytical expressions are developed to calculate instantaneous velocities without the need of generating velocity time history. Additionally, velocity spectra are expressed as a function of ambient turbulence intensity and an example is presented for a case where the spectra follows the five-thirds law. The presented approach is integrated into the numerical simulation using a circular grid that is discretized into multiple nodes.

TURBULENCE SIMULATION APPROACH

A statistical method of turbulence simulation similar to the one developed by Veers [7] is adopted. Since turbulent velocity at any given instant of time is desired for numerical simulation of turbine, a set of analytical expressions are developed to compute instantaneous flow velocity by treating the velocity as sine wave of multiple frequency components. The details of simulations approach for velocity in one direction is presented in [9] and extended here for velocities in all three direction.

Following are the main input parameters to calculate fluctuating velocity components: mean flow speed U, ambient Turbulence Intensity TI, minimum and maximum frequencies f_{min} and f_{max} within inertial subrange and correlation related parameters such as coherence decay constant C and factors P and Q relating standard deviations of velocity components. Kolmogorov's five-thirds law is utilized [10] and continuous power spectral density, $G(f)$, is calculated as a function of frequency, f, according to:

$$G(f) \propto f^{-\frac{5}{3}}, \quad (1)$$

which implies:

$$G^m(f) = A_m f^{-\frac{5}{3}}, \quad (2)$$

where A_m is a constant for a given TI and $m = u, v$ or w where u, v and w are velocity components in x, y and z directions respectively; and G^m is corresponding spectral density. The spectral density is found to follow Kolmogorov's five-thirds law at two tidal sites in Puget Sound, WA for frequency range at least within 0.2 Hz to 2 Hz [11]. For frequencies lower than 0.1 Hz, spectra were found to be less steep than within the inertial subrange but no mathematical relationship between spectra and frequency have been suggested [11]. If a suitable relationship between spectra and frequency is found for low frequencies ($f < 0.1$ Hz) for any given site, Equation 1 can be replaced by the appropriate

relationship without the loss of generality. The five-thirds law is just an example illustrated here.

In this paper, u is taken as the direction of stream-wise flow, v is cross-stream direction and w is vertical direction. The TI can be expressed as [12]:

$$TI = \frac{\sqrt{(\sigma_u)^2+(\sigma_v)^2+(\sigma_w)^2}}{\sqrt{\bar{u}^2+\bar{v}^2+\bar{w}^2}}, \quad (3)$$

where σ is standard deviation of velocity component represented by the subscript and $\bar{u}$, $\bar{v}$, and $\bar{w}$ are time averaged velocity components in x, y and z directions, i.e.. The magnitude of the average flow velocity is therefore $U = \sqrt{\bar{u}^2 + \bar{v}^2 + \bar{w}^2}$. The TI of component m, TI_m, is therefore given by:

$$TI_m = \frac{\sigma_m}{U}. \quad (4)$$

It is also noteworthy that$TI = \sqrt{(TI_u)^2 + (TI_v)^2 + (TI_w)^2}$.

The standard deviation, σ_m, is related to one sided power spectral density, $G^m(f)$, as [13]:

$$\sigma_m^2 = \int_0^\infty G^m(f)df. \quad (5)$$

To obtain an expression for A_m, Equation 5 is integrated over the inertial subrange, from frequency f_{min} to f_{max}, through incorporating Equations 1 and 4 in Equation 5. The expression for A_m is thus:

$$A_m = \frac{2U^2\, TI_m^2}{3\left[\frac{1}{f_{min}^{\frac{2}{3}}} - \frac{1}{f_{max}^{\frac{2}{3}}}\right]}. \quad (6)$$

Therefore, the power spectral density in the inertial sub-range can be written as:

$$G^m = \frac{2U^2\, TI_m^2}{3\left[\frac{1}{f_{min}^{\frac{2}{3}}} - \frac{1}{f_{max}^{\frac{2}{3}}}\right]} f^{-5/3}, \quad (7)$$

assuming the TI is derived from this same frequency range.

For any given velocity component in x, y or z direction, the flow between any two nodes i and j will be partially correlated. A coherence function Coh is utilized to correlate two nodes as [7]:

$$Coh_{ij} = \exp(-\frac{C\Delta r_{ij} f}{U}), \quad (8)$$

where Δr_{ij} is distance between nodes i and j, and C is a coherence decay constant.

The discretized cross spectral density between nodes i and j, S_{ij}^m, is related to Coherence function according to [7]:

$$S_{ij}^m(f) = 2Coh_{ij}\sqrt{S_{ii}^m(f)S_{jj}^m(f)}\,\delta f, \quad (9)$$

where $S_{ii}^m(f)$ is discretized power spectral density at node i, $S_{jj}^m(f)$ is discretized power spectral density at node j, Coh_{ij} is a coherence function between nodes i and j and δf is difference between two consecutive frequencies. It is noteworthy that $G^m = S^m\delta f$. The multiplier 2 on right hand side of Equation 9 is to ensure correct amplitude of sine wave developed in Equation 14 is maintained as amplitude of sine wave is twice its average power.

If auto-spectrum is assumed to be same for every location, i.e. $S_{ii}^m(f) = S_{jj}^m(f)$, Equation 9 can be expressed as:

$$S_{ij}^m = 2Coh_{ij}A_m\, f^{-\frac{5}{3}}\delta f. \quad (10)$$

Once the discretized cross spectral density is known, velocity weighing factor H can be calculated using Cholesky's decomposition as suggested in [7]:

$$\begin{aligned} H_{11} &= S_{11}^{1/2}, \\ H_{21} &= S_{21}/H_{11}, \\ H_{22} &= (S_{22} - H_{21}^2)^{1/2}, \\ H_{31} &= S_{31}/H_{11}, \quad (11) \\ &\vdots \\ H_{ij} &= (S_{ij} - \textstyle\sum_{l=1}^{l=j-1} H_{il}\ H_{jl})/H_{jj}, \\ H_{jj} &= \left(S_{jj} - \textstyle\sum_{l=1}^{l=j-1} H_{jl}^2\right)^{1/2}. \end{aligned}$$

The superscript m has been dropped from H and S in Equation 11 for clarity, however, it is noteworthy that Equation 11 is valid for any direction x, y or z.

Analytical expressions for velocity components

Random phase θ_{kl} associated with any frequency component f_k is generated for every node l. These random phases have equal probability of occurrence between 0 and 2π. Fluctuating velocity m_{kj}^* at node j as a function of frequency component f_k is then obtained similar to [7] as:

$$m_{kj}^* = \textstyle\sum_{l=1}^{j} H_{jl}^m\,(f_k)e^{i\theta_{kl}}. \quad (12)$$

It is seen that Equation 12 gives a complex value for u_{kj}^* whose resultant phase angle θ_{kj}^R can be determined as:

$$\theta_{kj}^R = \tan^{-1}\left(\frac{imag(m_{kj}^*)}{real(m_{kj}^*)}\right), \quad (13)$$

where $imag$ indicates that the imaginary part of m_{kj}^* is selected and $real$ indicates that the real part of m_{kj}^* is selected.

Equation 12 gives fluctuating velocity for all frequency components. In order to obtain the resultant fluctuating velocity in time domain at node j, the fluctuating velocity of every frequency component is treated as a sine wave and summed up. In other words, velocity $m_j(t)$ in time domain at node j for any instant of time t is obtained by as:

$$m_j(t) = \textstyle\sum_{k=1}^{k=N} m_{kj}^* \sin(2\pi f_k^* t + \theta_{kj}^R). \quad (14)$$

where N is total number of frequency discretization.

The relationship among standard deviations are left as user inputs and expressed as $\sigma_v = P\sigma_u$ and $\sigma_w = Q\sigma_u$. P and Q are constants and set as user inputs. Since TI and U are also user inputs, it is convenient to express σ_u as:

$$\sigma_u = \frac{TI\,U}{\sqrt{1+P^2+Q^2}}. \quad (15)$$

Cross-axis correlation exists among u, v and w components and effective instantaneous fluctuating velocity fluctuation in x-direction, $u_f(t)$, can be expressed as [8]:

$$u_f(t) = u(t) + r_{uv}v(t) + 2r_{uw}w(t), \quad (16)$$

where r_{uv} is cross-axis correlation between u and v and r_{uw} is cross-axis correlation between u and w.

Expressions for r_{uv} and r_{uw} for ocean environment are not available but adaptations from [8] as presented below are considered in this study:

$$r_{uv} = -0.136\sigma_u, \quad (17)$$

$$r_{uv} = -0.079\sigma_u - 0.325. \quad (18)$$

It is to be noted that fluctuating velocities obtained from Equation 14 averaged over time is 0 and the resultant velocity in x-direction (direction of flow), $u_R(t)$, at any time instant t is:

$$u_R(t) = \bar{u} + u_f(t). \quad (19)$$

TURBULENCE INTEGRATION IN TURBINE SIMULATION

Numerical simulation to predict performance of ocean current turbine was developed in [5] using unsteady Blade Element Momentum (BEM) rotor model for a turbine attached to a mooring cable. The simulation of the turbine with a 20 meter diameter variable pitch rotor presented by [6] was created using this rotor model and the turbulence approach described here is integrated in this simulation.

RESULTS

Turbulent flow is modeled using the method discussed above. Simulation is run for time period of 300 s with frequency discretized to 500 equal parts, $U = 1.6\,m/s$, $TI = 5\%$, $f_{min} = 0.01\,Hz$, $f_{max} = 5\,Hz$ and $C = 5$. The minimum and maximum frequencies chosen contain all inertial subrange frequencies measured in [11]. Furthermore, f_{min} is taken as 0.01 Hz in order to assess the effects of low frequencies. While low frequencies may not strictly follow five thirds law, this study attempts to find the order of effects by low frequencies and if a suitable mathematical relationship is found between spectra and low frequency, Equation 1 can be replaced while following the same approach. Figure 1 shows time history in the direction of flow. The time averaged velocity in the direction of flow is obtained from the simulation to be $\bar{u} = 1.6\,m/s$ and has a standard deviation of $\sigma_u = 0.052$. Here, values of P and Q taken are 0.8 and 0.5 respectively, therefore σ_u calculated from Equation 15 is 0.058. It is to be noted that the longer period of simulation with higher frequency discretization reduces the differences between calculated parameters from equations and simulation. For example, simulation run for 1000 s with frequency discretization of 1500 resulted in $\sigma_u = 0.057$.

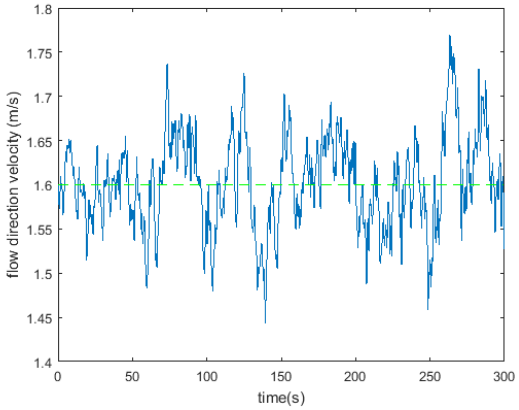

FIGURE 1. VELOCITY TIME HISTORY IN THE DIRECTION OF FLOW.

Figure 2 shows velocity time history in cross stream and vertical direction. The mean velocities $\bar{v}$ and $\bar{w}$ obtained from simulation are nearly equal to 0. Since the values of P and Q taken are 0.8 and 0.5 respectively, it is seen that fluctuation in cross stream direction is higher than in vertical direction. Velocity standard deviations in cross stream and vertical directions obtained from simulations are $\sigma_v = 0.045$ and $\sigma_w = 0.033$ whereas these values are 0.046 and 0.029 from target statistics based on values of P and Q. It is noteworthy that turbulent velocities obtained in Figures 1 and 2 obey continuity and conserve mass as the time averaged velocities in all three directions are not altered by the simulation.

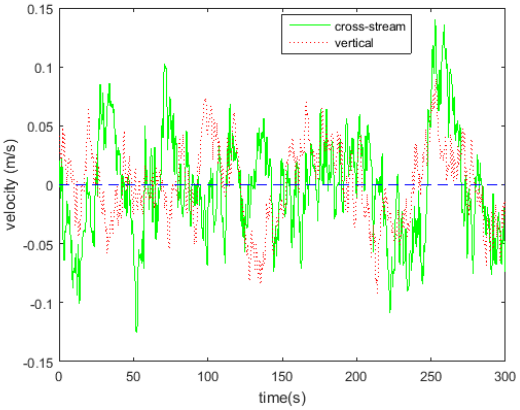

FIGURE 2. VELOCITY TIME HISTORY IN CROSS-STREAM AND VERTICAL DIRECTION.

Figure 3 shows color plot of a velocity in the direction of flow on a circular grid with azimuthal angles discretized to 16 equal parts and radius of circle discretized to 10 equal parts for an instantaneous time of $t = 5\ s$. The radius of circle is taken as 10m. This circular grid represents a rotor of radius 10 m where different patches of colors show different velocities throughout the rotor due to turbulence.

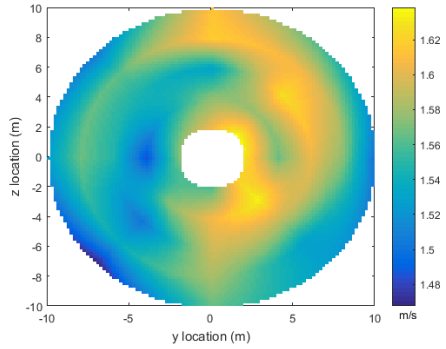

FIGURE 3. VELOCITY IN THE STREAMWISE DIRECTION FOR AN INSTANTENOUS TIME.

The turbulent flow modeling approach presented in this paper is also integrated in numerical simulation of OCT developed by SNMERC and presented in detail in [6]. Numerical simulations are carried out for calm seas, considering only one degree of freedom (blade rotation about rotor axis) so that turbine performance exclusively due to turbulence effects can be analyzed since perturbations due to wave and other motions are excluded. The simulation is carried out for a three bladed turbine with radius of 10 m.

Figure 4 shows results of numerical simulation for tip speed ratio (TSR) of 10.14 which is an optimum TSR; mean flow speed of 1.6 m/s; and $TI = 5\%$ and 20%. Site measurements in tidal channels in USA and Chile have indicated that TI varies between 5% and 20% [14] and these values are taken as reference here. The simulation is for time period of 1 hour. Figure 5 shows Power spectral density (PSD) of shaft power for $TI = 5\%$. The dotted line is a five- thirds line.

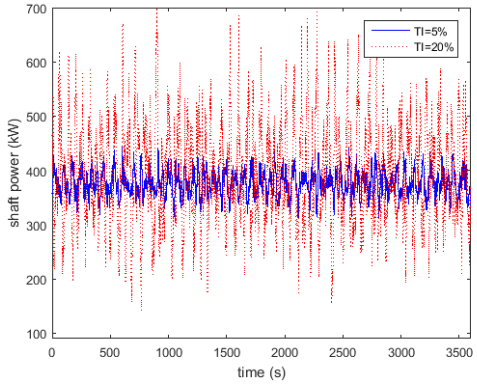

FIGURE 4. SHAFT POWER TIME HISTORY

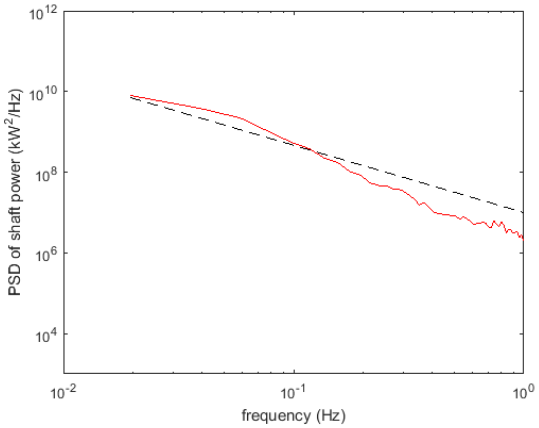

FIGURE 5. PSD OF SHAFT POWER FOR TI=5%.

Mean shaft power for $TI = 5\%$ and 20% are about 375.8 kW and 393 kW. It can be observed from Figure 4 that power fluctuation for TI of 20% is much higher than that of 5%. The standard deviations of shaft power for TI of 5% and 20% are 23.14 kW and 91.64 kW respectively. It is noteworthy that $TI = 20\%$ represents very high turbulence level where standard deviation is about 23% of mean power and may not be suitable for turbine installation unless control mechanism is adopted. Figure 5 shows that power spectra approximately follows the input five thirds law.

Figure 6 shows axial force variation in one blade of the tri-bladed rotor for $TI = 5\%$ and 20%. The mean forces for $TI = 5\%$ and 20% are 139.2 kN and 140.3 kN with standard deviations of 3.7 kN and 14.45 kN respectively. It can be observed that although the mean value has not increased greatly with increase in TI, the standard deviation for $TI = 20\%$ is nearly 4 times high than that for $TI = 5\%$. This indicates increase in fatigue load with TI. Figure 7 shows PSD of axial force on a blade of the tri-bladed rotor for $TI = 5\%$. The peak at frequency about 0.27 Hz is nearly equal to rotation frequency of turbine. It is also seen that axial force approximately follows the five-thirds law depicted by dotted line.

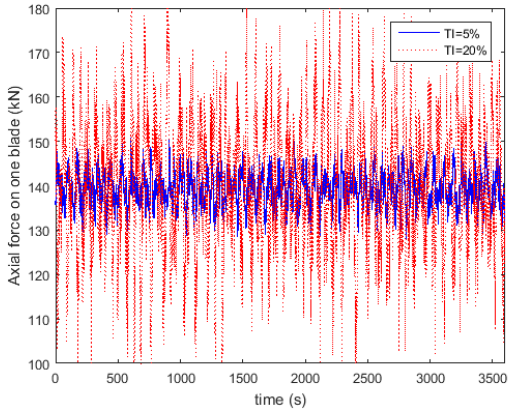

FIGURE 6. AXIAL FORCE ON ONE OF THE BLADES.

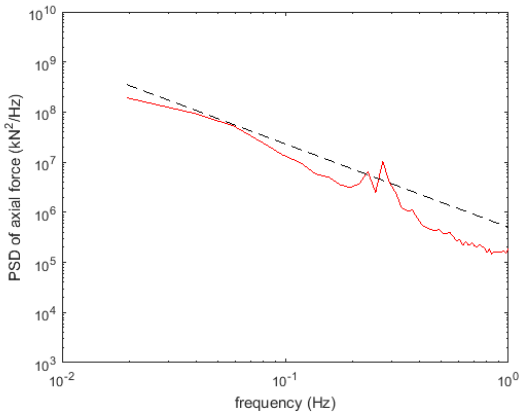

FIGURE 7. AXIAL FORCE SPECTRA ON ONE OF THE BLADES FOR TI=5%.

CONCLUSIONS

An approach to calculate turbulent flow velocity without having to generate velocity time history is presented to account for turbulence in numerical simulation of an ocean current turbine farm. The presented approach is integrated with numerical simulation of OCT developed by SNMREC. It is noted that although mean shaft power and mean axial force on a blade do not vary greatly with change in ambient turbulence intensities, the fluctuation of these parameters about their corresponding mean values are higher for higher ambient turbulence intensities. This means fatigue load on turbine blade increases with increase in turbulence level.

ACKNOWLEDGEMENTS

We would like to thank the National Science Foundation (NSF) and specifically the Energy, Power, Control and Networks (EPCN) program for their valuable ongoing support in this research within the framework of grant ECCS-1308168 'Collaborative Research: Optimized Harvesting of Hydrokinetic Power by Ocean Current Turbine Farms Using Integrated Control'. SNMREC is supported by the U.S. Department of Energy and the State of Florida.

REFERENCES

[1] GeorgiaTech Research Corp., 2013, "Assessment of Energy Production Potential from Ocean Currents along the United States Coastline," Atlanta, GA.

[2] U.S. Energy Information Administration, 2015, "Annual Energy Review," < http://www.eia.gov/>

[3] Machado, M.C.P.M. , VanZwieten, J.H., Pinos, I., 2016, "A Measurement Based Analyses of the Hydrokinetic Energy in the Gulf Stream," Journal of Ocean and Wind Energy, 3(1), 25-30.

[4] VanZwieten, J., McAnally, W., Ahmad, J., Davis, T., Martin, J., Bevelhimer, M., Cribbs, A., Lippert, R., Hudon, T., and Trudeau, M., 2014, "In-Stream Hydrokinetic Power – A Review and Appraisal," Journal of Energy Engineering, no. 04014024.

[5] VanZwieten Jr, J. H., Vanrietvelde, N., and Hacker, B.L., 2013, "Numerical Simulation of an Experimental Ocean Current Turbine," IEEE Journal of Oceanic Engineering, Vol. 38, No. 1, pp. 131-143.

[6] VanZwieten, J.H., Pyakurel, P., Ngo, T. , Sultan, C., Xiros, N.I., (TBD) "An assessment of using variable blade pitch for moored ocean current turbine flight control" Accepted to International Journal of Marine Energy.

[7] Veers, P.S., "Three-Dimensional Wind Simulation," Sandia National Laboratories, 1988.

[8] Kelley, N. D., 1992, "Full vector (3-D) inflow simulation in natural and wind farm environments using an expanded version of the SNLWIND (VEERS) turbulence code", NREL.

[9] Pyakurel, P., VanZwieten, J. H., Ananthakrishnan, P., Tian, W., accepted for publication, 2016, "Simulating turbulence for ocean current turbine", 21st SNAME Offshore Symposium, Houston, February 2016.

[10] Hunt, J.C.R., and Vassilicos, J.C., 1991, "Kolmogorov's Contributions to the Physical and Geometrical Understanding of Small-Scale Turbulence and Recent Developments", Royal Society Publishing, Proceedings: Mathematical and Physical Sciences, Vol. 434, No. 1890, Turbulence and Stochastic Process: Kolmogorov's Ideas 50 Years On, Jul. 8, 1991, pp. 183-210.

[11] Thomson, J., Polagye, B., Durgesh, V., and Richmond, M. C., 2012, "Measurements of Turbulence at Two Tidal Energy Sites in Puget Sound, WA", IEEE Journal of Oceanic Engineering, Vol. 37, No. 3, July 2012.

[12] Maganga, F., Germain, G., King, J., Pinon, G., and Rivoalen, E., 2010, "Experimental characterisation of flow effects on marine current turbine behaviour and on its wake properties," IET Renewable Power Generation, Volume 4, Issue 6, pp. 498–509.

[13] Jonkman, B., and Kilcher, L., 2012, "Turbsim User's Guide: Version 1.06.00," NREL.

[14] Thomson, J., Kilcher, L., Richmond, M., Talbert, J., deKlerk, A., Polagye, B., Guerra, M., Cienfuegos, R., 2013, "Tidal turbulence spectra from a compliance mooring", Proceedings of the 1st Marine Energy Technology Symposium, METS2013, April 10-11, 2013, Washington, D.C.